Journal of Marine Science and Technology

Volume 27 | Issue 3 Article 4

OPTIMUM ARRANGEMENT OF NAVY SHIP EQUIPMENT FOR RADAR CROSS SECTION REDUCTION

Joon-Tae Hwang
Department of Naval Architecture and Ocean Engineering, Seoul NationalUniversity, Seoul, Korea.Research Institute of Marine Engineering, Seoul NationalUniversity, Seoul,Korea

Suk-Yoon Hong
Department of Naval Architecture and Ocean Engineering, Seoul NationalUniversity, Seoul, Korea.Research Institute of Marine Engineering, Seoul NationalUniversity, Seoul,Korea

Jee-Hun Song
Department of Naval Architecture and Ocean Engineering, Chonnam National University, Yeosu, Korea., jhs@jnu.ac.kr

Hyun-Wung Kwon
Department of Shipbuilding & Marine Engineering, Koje College, Koje, Korea.

OPTIMUM ARRANGEMENT OF NAVY SHIP EQUIPMENT FOR RADAR CROSS SECTION REDUCTION

Acknowledgements

This research was supported by the Research Institute of Marine Systems Engineering and Basic Science Research Program through the National Research Foundation of Korea (NRF) funded by the Ministry of Education, Science and Technology (2016R1D11A1A09918294, 2015R1D1A1A01060387).

Journal of Marine Science and Technology, Vol. 27, No. 3, pp. 220-228 (2019)
DOI: 10.6119/JMST.201906_27(3).0004

OPTIMUM ARRANGEMENT OF NAVY SHIP EQUIPMENT FOR RADAR CROSS SECTION REDUCTION

Joon-Tae Hwang[1, 2], Suk-Yoon Hong[1, 2], Jee-Hun Song[3], and Hyun-Wung Kwon[4]

Key words: radar cross section (RCS), stealth technology, radar absorbing structure (RAS) method, equipment arrangement design, advanced navy ship.

ABSTRACT

Multiple reflections on navy ship equipment cause unexpectedly high radar cross-section (RCS) distributions based on the location of each equipment on the ship. No RCS reduction method has been considered to date because the directions of re-radiated electromagnetic waves are difficult to predict. In this study, an equipment arrangement design system for navy ships was developed to minimize RCS to reduce the radar detection range of naval ships by the enemy. To minimize the possibility of operating range interferences among equipment, optimal equipment arrangement areas and operation ranges were determined with reference to real navy ships. Various arrangements were tested by using a genetic algorithm (GA) to find the optimal positions with minimum RCS values within the areas of each equipment. Further, the radar detection range was considered from the perspective of survivability.

I. INTRODUCTION

When it comes to modern naval warfare, the probability of detection is an important factor that determines survivability. Stealth technology is one of the most effective methods to decrease the probability of detection of naval ships. The radar-cross-section (RCS) reduction is a major feature of the stealth technology. The most effective RCS reduction technology is the radar-absorbing-structure (RAS) method, which involves the shape design and application of shielding to simplify complex targets. The RAS method involves changing the direction of electromagnetic waves to a direction different from that of the radiated electromagnetic waves. Various studies have been conducted on the RAS method, such as the RCS distribution analysis, studies on the shape design and shielding of equipment, and utilization of the advanced enclosed mast (AEM) and integrated mast module (IMM) systems to simplify the shapes of antennas and sensors (Park, 2004; Kim et al., 2011; Kwon et al., 2014a; Shin et al., 2017; Wang et al., 2017).

Another way to reduce the RCS is by using a radar-absorbing material (RAM) after the design stage. The RAM has electromagnetic properties and can absorb electromagnetic waves. It is produced with a lossy filler, which absorbs electromagnetic waves, and elastic materials such as rubber sheets. Furthermore, by using a genetic algorithm, multi-objective function optimization techniques have been applied to design multi-layered wide-band electromagnetic wave absorbers (Park et al., 2004; Saville, 2005; Goudos, 2007; Kwon et al., 2014b).

Recently, research on the absorber technology has advanced, and the use of artificially structured electromagnetic wide-band structural absorbers has become more common. The structural absorber functions through an electromagnetic resonance mechanism, in which the electric and magnetic responses can be independently tuned and the impedance of the structure can be matched to that of free space by modifying the geometry of the unit cell (Cheng et al., 2012; Fan et al., 2012).

Navy ships are heavily equipped for naval warfare with front guns, missiles, radar systems, and so on. Most equipment on these ships have complex shapes, which causes extremely high RCS distributions. While the RCS values vary with the location of the ship equipment, no RCS reduction method has yet been considered because the directions of re-radiated electromagnetic waves are difficult to predict.

In this study, an equipment arrangement design system was developed to minimize the RCS to reduce the range for radar detection of the navy ships by the enemy. To demonstrate the application of the arrangement design system, an LCS-2 type model was selected. A front gun, seaRAM (rolling airframe missile), radar, and sensor each were set up as the equipment in the model.

Paper submitted 10/15/18; revised 12/17/18; accepted 04/19/19. Author for correspondence: Jee-Hun Song (e-mail: jhs@jnu.ac.kr).
[1] *Department of Naval Architecture and Ocean Engineering, Seoul National University, Seoul, Korea.*
[2] *Research Institute of Marine Engineering, Seoul National University, Seoul, Korea.*
[3] *Department of Naval Architecture and Ocean Engineering, Chonnam National University, Yeosu, Korea.*
[4] *Department of Shipbuilding & Marine Engineering, Koje College, Koje, Korea.*

To minimize the possibility of the operating range interference among equipment, their arrangement areas and operation ranges were determined with reference to those of previous navy ships. The optimal arrangement design of the equipment was determined considering multiple reflections by using a genetic algorithm (GA) to find positions that will result in the minimum RCS value within the area of each equipment.

II. THEORETICAL BACKGROUND

1. Radar Cross Section

The radar cross section is an important parameter of an active radar equation and indicates the echo of targets. It is a parameter that indicates the ratio of the re-radiated wave intensity to the incident wave intensity. More precisely, it is the limit of that ratio as the distance from the scatterer to the point where the scattered power is measured approaches infinity. In other words, the RCS is an area that intercepts the incident intensity in the intuitive sense. The definition of RCS is given as the following equation:

$$\sigma = \lim_{R\to\infty} 4\pi R^2 \frac{|E_s|^2}{|E_i|^2} \tag{1}$$

where σ is the RCS, E_s is the electric vector scattered from the target, E_i is the incident electric vector on the target surface, and R is the distance between the receiver and the center of the target.

2. Representative Value of RCS

The representative value to be applied to the RCS analysis can be defined as follows within the azimuth range. The average value of the RCS in the azimuth range, the median value of the RCS value when the RCS is sorted in ascending order, and the maximum value, which is the maximum RCS value among the RCS values. There are some differences in the performance evaluation according to the selection criterion. It is reasonable to apply it as the average value considering the data processing method of the RCS measurement and the radar target detection principle. The meaning of the mean value is to calculate the decibel (dB) per square meter after taking an average in the RCS defined in square meters. dB is a method for effectively indicating when the dynamic range is very large, mainly in a linear value. dB is a unit of symmetrical representation of + and − values based on RCS value 1-m^2 and uses log function as follows.

$$RCS = 10\log_{10}\sigma(\text{dB}) \tag{2}$$

3. Consideration of the Visual Surface of the Target

The RCS analysis of complex equipment, those that are not visible from the observation point of the radar, should be excluded from the study to obtain accurate results. Therefore, to determine the visible area with respect to the radar, we first used the back-face-culling method to remove the equipment facing away from the radar. The back-face-culling method interprets only parts excluded from the analysis when the normal vector to the plate is in the negative x-direction and the incident wave is in the positive x-direction; that is, when the inner product of the incident wave vector and the normal vector to the plate is smaller than zero, the plate is removed, as shown by the dash line in Fig. 1(a). Second, we used the adaptive triangle method, which is a hidden surface removal method. When an element partially obscured by the A-plane is sequentially divided into extended triangles, as shown by the dotted lines in Fig. 1(b), with a vertex on the A-plane and another at the intersection, the depth test can be performed to distinguish between the visible and hidden surfaces.

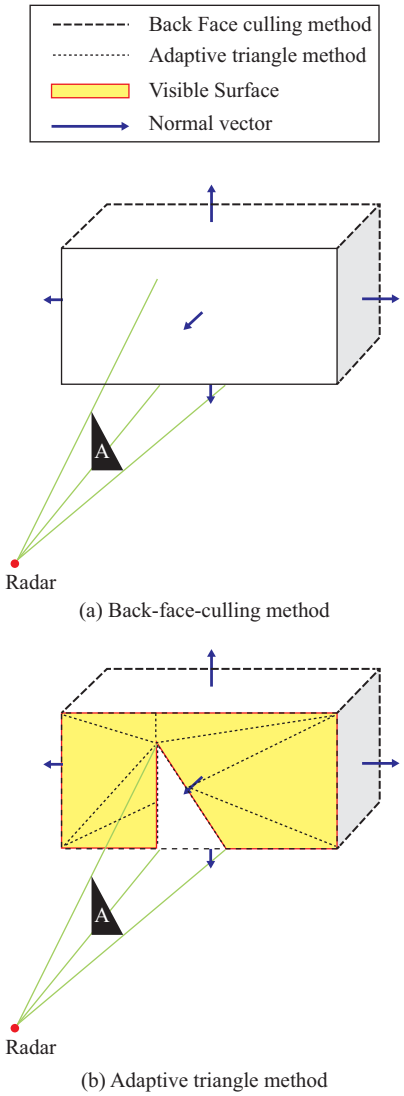

Fig. 1. Hidden surface determination.

4. Consideration of Multiple Reflections of Targets

Multiple reflections on targets with complex shapes have high distributions that are not negligible. To consider multiple reflections on equipment with complex shapes, a combination of

geometric optics (GO) and physical optics (PO) methods was used. The GO method was applied to find the paths of the multiple-reflection waves, and PO was applied to the last reflection.

The theory of PO overcomes the catastrophe of the infinities on flat and singly curved surfaces by approximating the induced surface fields and integrating them to obtain the scattered field.

Assuming that the electromagnetic wave incident to a target is a plane wave, we can calculate $\vec{E}_s$, which is the electric vector scattered from the target, using the following Stratton-Chu integral equation (Stratton, 1941).

$$\vec{E}_s = -\frac{jke^{-jkR}}{2\pi R}\hat{\zeta}_s \times \int_S \left\{\hat{n}\times\vec{E} - \eta\hat{\zeta}_s \times (\hat{n}\times\vec{H})\right\} e^{jk\vec{r}\cdot(\hat{\zeta}_s - \hat{\zeta}_i)} dS \quad (3)$$

where $\hat{n}$ is the unit normal vector of the target surface, $\vec{E}$ and $\vec{H}$ are the electric and magnetic field vectors induced on the surface, $\hat{\zeta}_i$ and $\hat{\zeta}_s$ are the unit directional vectors of the incidence and scattering of the electromagnetic wave, and η is the impedance of the medium. We obtain the scattering electric field vector $\vec{E}_s$ using the following equation:

$$\vec{E}_s = -\frac{jke^{-jkR}}{2\pi R} E_0 \vec{W}(\hat{p}) \int_S e^{jk\vec{r}\cdot(\hat{\zeta}_s - \hat{\zeta}_i)} dS \quad (4)$$

where E_0 is the magnitude of the incident electric field vector and $\vec{W}(\hat{p})$ is a polarization vector with respect to the unit polarization vector $\hat{p}$. $\vec{W}(\hat{p})$ is represented by the following equation:

$$\vec{W}(\hat{p}) = \frac{1}{2}\hat{\zeta}_s \times \left[(1+R_E)(\hat{p}\cdot\hat{e}_\perp)(\hat{n}\cdot\hat{e}_\perp) + (1-R_H)(\hat{p}\cdot\hat{e}^i_\parallel)(\hat{\zeta}_i\cdot\hat{n})\hat{e}_\perp + (1-R_E)(\hat{p}\cdot\hat{e}_\perp)(\hat{\zeta}_i\cdot\hat{n})(\hat{\zeta}_s\cdot\hat{e}_\perp) - (1+R_H)(\hat{p}\cdot\hat{e}^i_\parallel)\{\hat{\zeta}_s\times(\hat{n}\times\hat{e}_\perp)\}\right] \quad (5)$$

where R_H and R_E are the Fresnel reflection coefficients for H- and E-polarizations, respectively.

The GO method is a ray-tracing procedure in which the wavelength is allowed to become an infinitesimally small ray tube. In the high frequency range, it is assumed that an electromagnetic wave propagates in a straight path and reflects in the specular direction in a homogeneous medium. The directions of the scattering unit vector, $\hat{\zeta}_s$, and specular reflection vector, $\hat{\zeta}_r$, coincide according to Snell's law. The polarization vector, $\vec{W}(\hat{p})$ can be simplified to the following equation (Knott, 1993):

$$\vec{W}(\hat{p}) = -\left\{R_E(\hat{p}\cdot\hat{e}_\perp)\hat{e}_\perp + R_H(\hat{p}\cdot\hat{e}^i_\parallel)\hat{e}^r_\parallel\right\}(\hat{\zeta}_r\cdot\hat{n}) \quad (6)$$

Using a combination of the GO and PO methods, the reflected paths and effective area can be determined, as shown in Fig. 2.

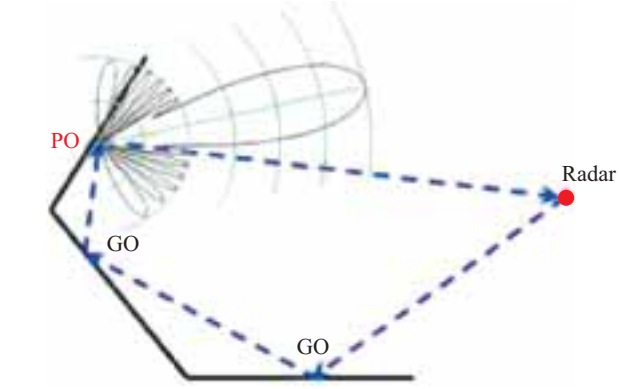

(a) Multiple reflection paths

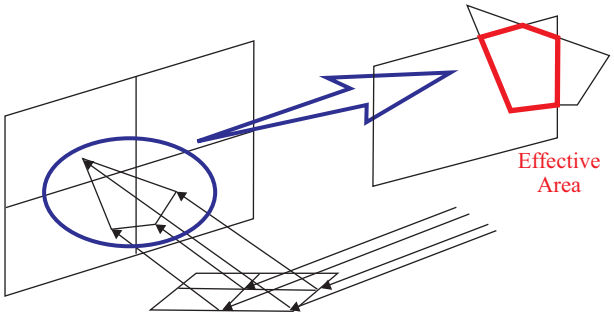

(b) Effective area

Fig. 2. Concept of multiple reflections.

5. Radar Detection Range

In modern navy military weapon systems, decreasing the detection range for the enemy or active-guided missiles can improve the survivability of navy ships. The following equation is used to calculate the radar detection range of a navy ship (Richards et al., 2010).

$$R_{\max} = \sqrt[4]{\frac{P_t G\sigma Ae}{(4\pi)^2 S_{\min}}} \quad (7)$$

where P_t is the transmitted power (watt), G is the antenna gain (ratio), σ is the target RCS area (m^2), A_e is the antenna aperture (m^2) and $S_{\min}$ is the minimum detectable signal at the receiver (watt). Fig. 3 shows the change in the detection ranges with a decrease in the RCS when other parameters were fixed. When the RCS decreased by 3 dB, the detection range decreased by approximately 16%.

III. EQUIPMENT AND FUNCTIONS OF AN EQUIPMENT ARRANGEMENT DESIGN SYSTEM

The optimal equipment arrangement design system for a navy ship consists of two major parts: the RCS analysis module

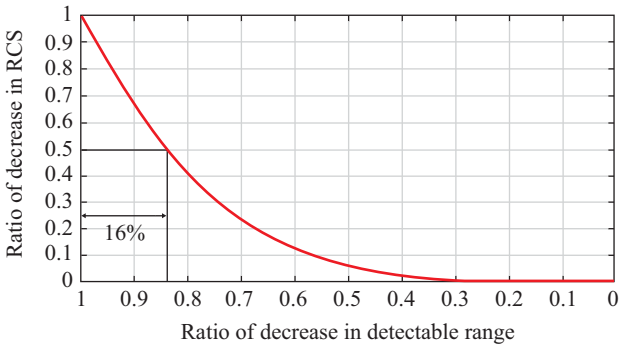

Fig. 3. Ratio of decrease in detection range versus ratio of decrease in RCS.

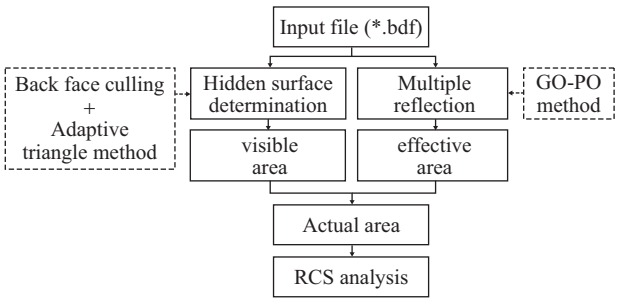

Fig. 4. The RCS analysis module.

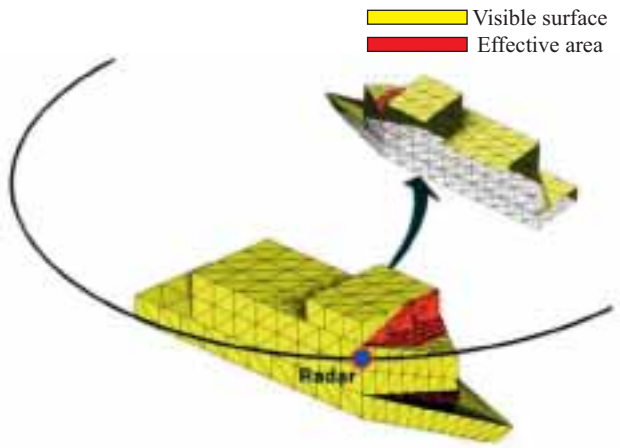

Fig. 5. Visible surface and effective area of the simplified ship model according to the location of the radar.

and the optimal arrangement design analysis module. The features and equipment corresponding to each of these modules are described in the following subsections.

1. RCS Analysis Module

To obtain accurate results, equipment or parts of equipment that are not visible from the observation points at the radar should be excluded from the RCS analysis. Therefore, to determine the actual area for the RCS analysis, we used an RCS analysis module consisting of hidden surface determination and multiple reflections, as shown in Fig. 4. We used the back-face-culling

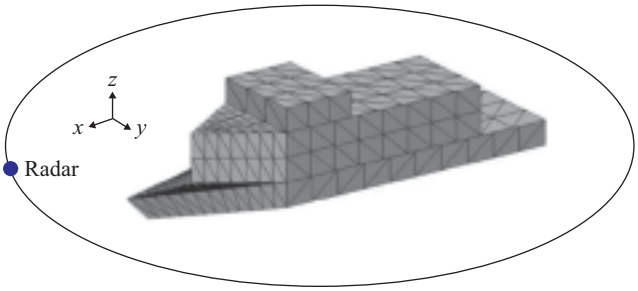

Fig. 6. The simplified ship model.

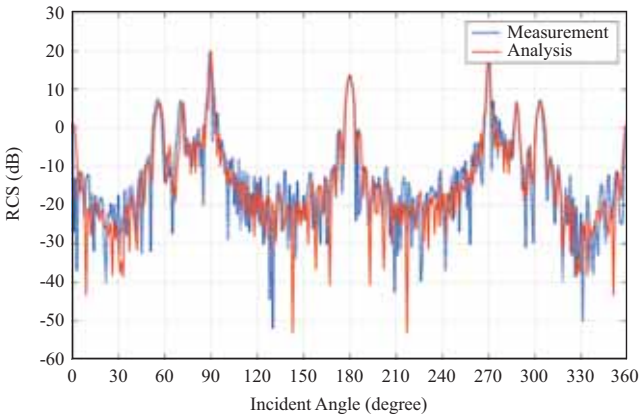

Fig. 7. Comparison between measured data of the simplified ship model and analysis results when f = 10 GHz.

and adaptive triangle methods to determine the hidden surface. Further, the multiple reflection effect of the radar was considered by using GO and PO methods in combination. Fig. 5 shows examples of the visible surface and effective area in the simplified ship model with respect to the location of the radar.

1) Verification Using a Simplified Ship Model

To demonstrate the RCS analysis module, we performed an RCS analysis using a simplified ship model and compared our results with the measurement data (Park, 2004). Fig. 6 shows the simplified ship model consisting of 686 elements with $0.9 \times 0.2 \times 0.2$ (m). The measurement and analysis conditions were the same, with a 10 GHz frequency and a 5 m distance between the radar and the simplified ship model. Fig. 7 shows a comparison of the measurement data of the simplified ship model with the results obtained through the RCS analysis module. The results show that the measurement of a complex target is consistent with the numerical solution for a meshed model.

2. Optimum Arrangement Design Analysis Module

To minimize the possibility of the operating range interference among equipment, the optimal arrangement of equipment and their operation ranges were determined based on actual navy ships. We used a GA to determine the optimal arrangement by taking multiple reflections into account. Fig. 8 shows the optimal arrangement determination procedure based on using a GA.

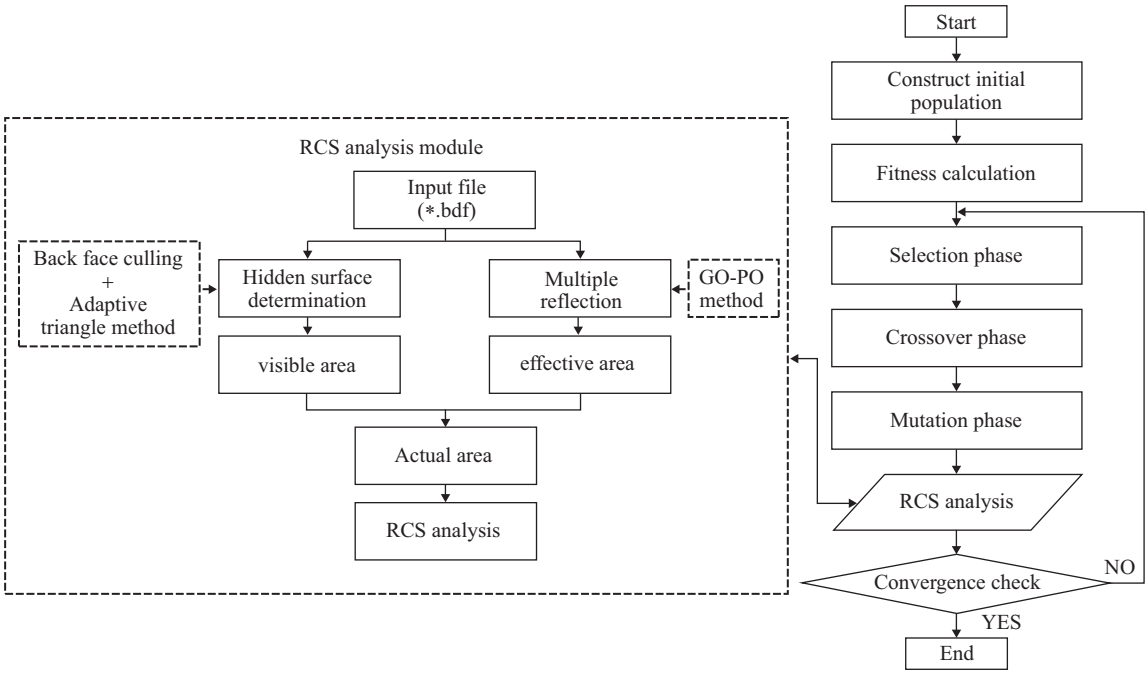

Fig. 8. Optimal arrangement procedure using GA.

As shown in Fig. 8, the fitness of each individual in the population can be evaluated in the first generation. Then, two individuals with good fitness can be selected as parents to produce new individuals. Further, new generations can be procured by repeating the evaluation, selection, crossover, and mutation processes, and the RCS analysis can be performed. The design variables and constraints are that the arrangement in the set-up arrangement area and the operating ranges of the equipment do not interfere with other structures. The convergence criterion of a genetic algorithm is the maximum number of iterations that reach a predefined value. The predefined value is 10,000 and performed iterative analysis using genetic algorithm until this number is reached. In this study, the RCS analysis was performed using the RCS analysis module whose verification is discussed in Section 3.1. The optimal arrangement design can be determined by repeating this procedure. However, repeated RCS analyses of new generations of overlapping elements incur unnecessary analysis costs. Therefore, for each new generation, we performed a partial analysis of only the changed elements; whereas, for unchanged elements, we used the RCS analysis results of the current generation

3. GUI Program for Equipment Arrangement Design System

The GUI program was written with resources from Microsoft Visual Studio of C#, a well-known Windows programming tool kit. A user can directly control the program flow by selecting appropriate menus. The GUI layout of the program is shown in Fig. 9. The main window consists of 3D visualization, RCS analysis module, and exterior structure arrangement module. The 3D visualization window is used to display the geometric shape of numerical models and model data files from the generalized CAD software MSC/PATRAN(*.bdf). The calculation options available in the RCS analysis module include the radar frequency, distance from the target, range of azimuth, and vertical angle. The exterior structure arrangement module sets the arrangement area and operation range of each exterior structure.

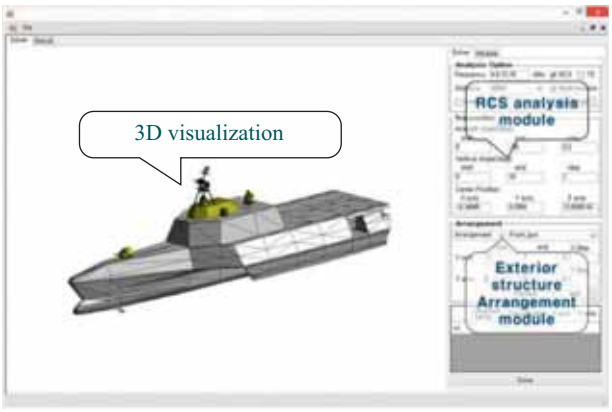

Fig. 9. The GUI layout.

IV. APPLICATION TO A NAVY SHIP

In this study, we focused on determining the optimal equipment arrangement design to minimize multiple reflections and the RCS to reduce the detection range by the enemy. For use with other design variables, ten cases each of optimal and worst arrangement designs were derived to enable the selection of optimal cases satisfying all design variables.

To demonstrate the application of the program, an LCS-2

Table 1. Specifications of LCS-2 type model equipped front gun, seaRAM, radar and sensor model.

Model	Length	Width	Height	Element number
LCS-2	127 m	31.6 m	22.8 m	5,012
Front gun	6.5 m	3.3 m	3.0 m	312
Sensor	2.3 m	2.3 m	2.5 m	126
Radar	17.2 m	7.3 m	15.0 m	1,242
SeaRAM	3.0 m	2.5 m	4.3 m	254

Table 2. Coordinates of arrangement areas and operation ranges of front gun, sensor, radar, seaRAM.

Exterior Equipment	x-coordinate of arrangement area		Step	y-coordinate of arrangement area		Step	Operation range	
	Start	End		Start	End		Min	Max
Front Gun	16 m	40 m	0.1 m	-	-	-	-10°	77°
SeaRAM	70 m	81 m	0.1 m	-	-	-	-	-
Radar	60 m	65 m	0.1 m	-	-	-	-	-
Sensor	60 m	68 m	0.1 m	4.5 m	6 m	0.1 m	70°	90°

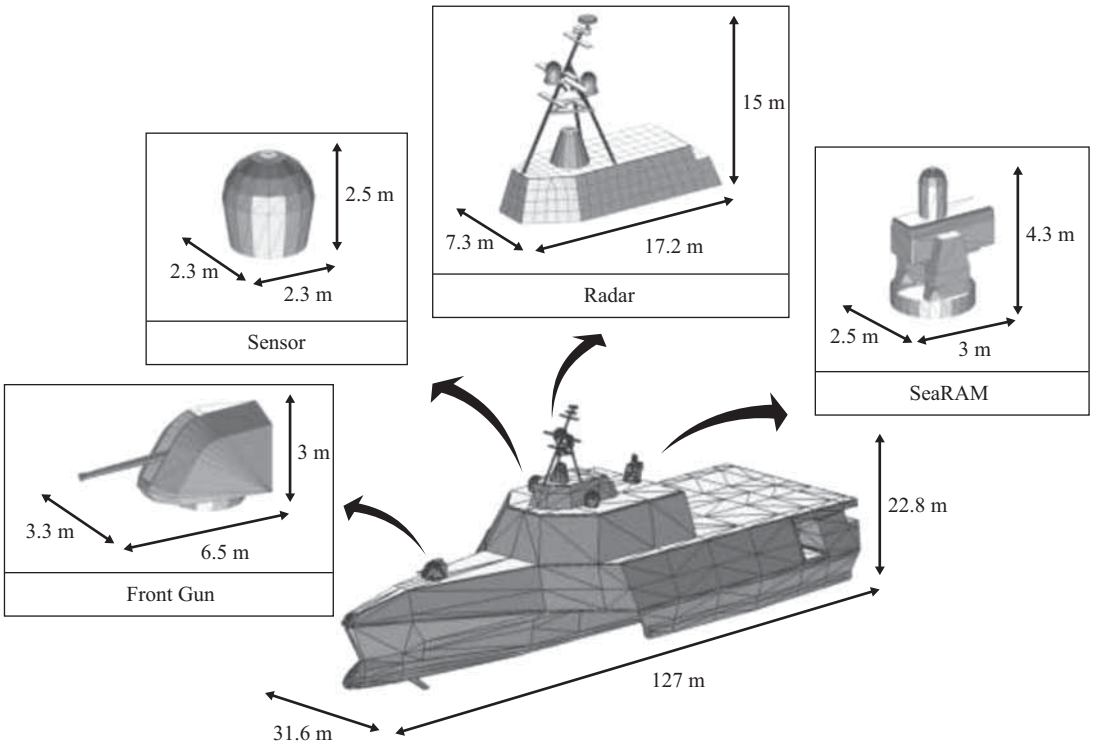

Fig. 10. LCS-2 type model equipped with front gun, sensor, radar and seaRAM.

type model was selected and a front gun, seaRAM, radar, and sensor were used as the model equipment. Fig. 10 and Table 1 show the analysis model and its specifications. We set the RCS mean values for the index of the optimal positions, and the range of the azimuth angle varied from 0 to 180 degrees in 0.2-degree steps owing to the symmetry of shapes.

1. Arrangement Areas of Equipment

In the first step, we set the arrangement areas and operation ranges of equipment parts. The arrangement areas were set with reference to the navy ship LCS-2, and the operation ranges of the front gun, sensor, radar, and seaRAM were determined with reference to the specifications of MK-110, UHF SATCOM, SeaGIRAFFE AMB, and MK-15 SeaRAM. While Fig. 11 shows the arrangement areas and coordinates of the front gun, sensor radar, and seaRAM, Table 2 shows the coordinates of the arrange-

Table 3. RCS mean values and coordinates of the ten cases each of optimal and worst arrangement positions for front gun, seaRAM, radar, and sensor.

	RCS mean value	Front gun		SeaRAM		Radar		Sensor	
		x	y	x	y	x	y	x	y
Optimal arrangement									
Case 1	23.11 dB	22.2 m	-	77.8 m	-	63.3 m	-	60.2 m	4.3 m
Case 2	23.15 dB	21.9 m	-	77.9 m	-	63.5 m	-	61.1 m	4.5 m
Case 3	23.12 dB	19.0 m	-	79.4 m	-	64.8 m	-	62.0 m	5.0 m
Case 4	23.13 dB	18.7 m	-	79.8 m	-	65.3 m	-	60.6 m	5.5 m
Case 5	23.14 dB	21.3 m	-	80.0 m	-	65.6 m	-	67.5 m	5.7 m
Case 6	23.16 dB	19.4 m	-	80.3 m	-	65.7 m	-	66.3 m	5.8 m
Case 7	23.15 dB	19.0 m	-	80.1 m	-	65.6 m	-	64.0 m	5.5 m
Case 8	23.12 dB	19.1 m	-	78.5 m	-	64.0 m	-	63.3 m	5.4 m
Case 9	23.15 dB	19.2 m	-	80.8 m	-	66.2 m	-	63.8 m	5.2 m
Case 10	23.14 dB	18.9 m	-	78.0 m	-	63.5 m	-	61.2 m	4.7 m
Worst arrangement									
Case 1	26.61 dB	34.2 m	-	74.2 m	-	62.2 m	-	61.1 m	4.1 m
Case 2	26.50 dB	35.2 m	-	74.5 m	-	62.6 m	-	60.3 m	4.8 m
Case 3	26.42 dB	33.3 m	-	77.4 m	-	65.4 m	-	63.9 m	5.7 m
Case 4	26.33 dB	35.3 m	-	75.3 m	-	63.3 m	-	62.4 m	4.6 m
Case 5	26.54 dB	38.9 m	-	76.1 m	-	65.7 m	-	63.1 m	4.1 m
Case 6	26.25 dB	37.6 m	-	76.5 m	-	66.0 m	-	66.6 m	5.8 m
Case 7	26.24 dB	33.2 m	-	75.5 m	-	63.6 m	-	67.2 m	5.0 m
Case 8	26.25 dB	38.2 m	-	78.2 m	-	66.2 m	-	62.4 m	5.4 m
Case 9	26.25 dB	33.9 m	-	77.9 m	-	66.0 m	-	61.2 m	5.3 m
Case 10	26.24 dB	38.2 m	-	78.0 m	-	67.5 m	-	61.5 m	4.9 m

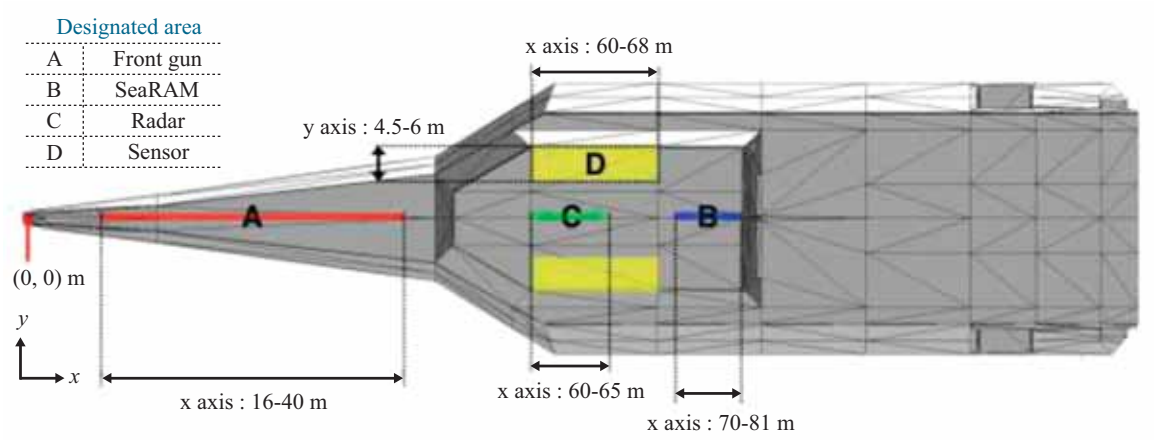

Fig. 11. Arrangement areas and coordinates of front gun, seaRAM, radar and sensor.

ment areas and operation ranges for these equipment. Each equipment has a operating range and should not interfere with other equipment and structures. We only considered the x-axis of the arrangement areas for the front gun, radar, and seaRAM because of the symmetry of the model.

1. Analysis of Arrangement Design for the Selected Equipment

In the second step, by using a GA, we performed optimization of the arrangement design for the equipment in the arrangement areas mentioned in section 4.1. To derive the optimal arrangement areas for use with other design variables, ten analyses each were performed for the optimal and worst arrangements. Fig. 12 and Table 3 show ten cases each of optimal and worst cases for the coordinates of the equipment and the RCS mean values of the front gun, SeaRAM, radar, and sensor. As shown in Fig. 12 and

Table 4. Distance between SeaRAM and Radar in optimal and worst arrangement cases.

	Distance between SeaRAM and Radar	
	Optimal arrangement	Worst arrangement
Case 1	14.5 m	12.0 m
Case 2	14.4 m	11.9 m
Case 3	14.6 m	12.0 m
Case 4	14.5 m	12.0 m
Case 5	14.4 m	10.4 m
Case 6	14.6 m	10.5 m
Case 7	14.5 m	11.9 m
Case 8	14.5 m	12.0 m
Case 9	14.6 m	11.9 m
Case 10	14.5 m	10.5 m

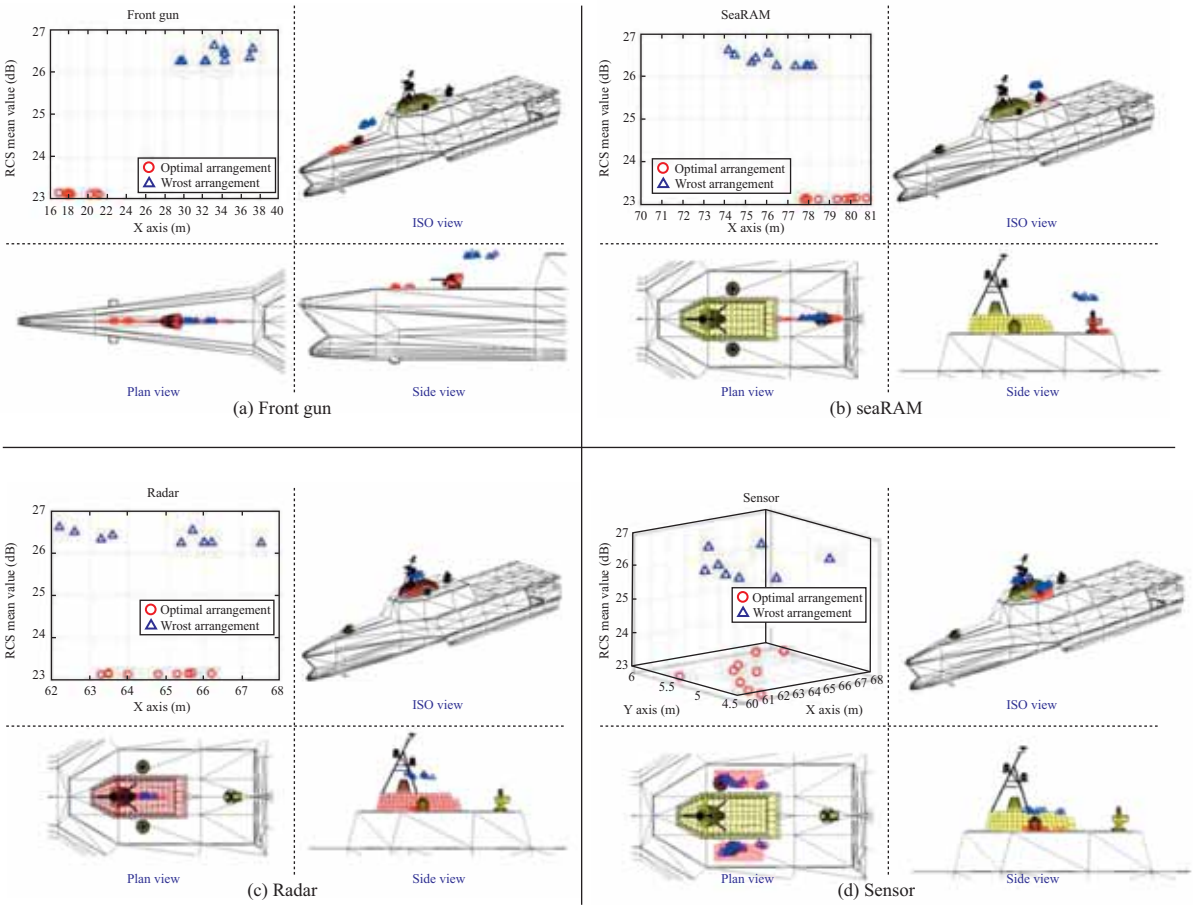

Fig. 12. Arrangement positions and RCS mean values of the equipment.

Table 3, the front gun is not affected by the other equipment and shows optimal results on the x-axis at approximately 18-19 m and 21-22 m. The worst cases can be seen on the x-axis at approximately 33-35 m and 37-38 m; and it can be seen that they are close to the bridge. Since the seaRAM and radar are adjacent to each other, we considered the distance between these equipment. Table 4 shows the distance between the seaRAM and radar for 10 cases each of optimal and worst cases. We can see that the two are spaced approximately 14.5 m apart in all optimal cases. In the worst cases, they are spaced by approximately 10.5 m and 12 m. It can be seen that the arrangement positions are all different, but the spacing remains the same. From this result, it can be seen that it is better to keep the distance between the equipment at 14.5 m. In the case of the sensor, it is also ad-

jacent to the radar, but the arrangement positions were not specified between the optimal and the worst arrangements. From this result, it can be seen that the sensor has a small RCS contribution, so it can be placed at any position. From Table 3, it can be seen that the RCS mean values of the optimal and worst arrangement positions differ by about 3 dB. In modern navy military weapon systems, the detectability of the ship is closely related to its survivability. Therefore, when the RCS is reduced by 3 dB, the ratio of decrease in the detection range is 16%.

V. CONCLUSIONS

In this study, an equipment arrangement design system was developed to minimize the equipment RCS to reduce the detection range of naval ships by the enemy. Using a GA, an arrangement design of the equipment was designed to find optimal positions with minimum RCS values in the arrangement areas set for each equipment. To minimize the possibility of the operating range interference among equipment, their optimal equipment arrangement areas and operation ranges were designed with reference to actual navy ships. Ten cases each of optimal and worst arrangement positions of the equipment were derived for use with other design variables. Finally, the optimal cases satisfying the other design variables were selected and the worst cases were avoided.

To demonstrate the application of the program, an LCS-2 type model was selected and a front gun, seaRAM, radar, and sensor were set up as the model equipment. The RCS mean values of the optimal and worst arrangement positions differ by about 3 dB. The ratio of decrease in the detection range is 16%. These results indicate that the optimal arrangement design of the equipment, considering multiple reflections, determined in this study is applicable to navy ships and could be used as an RAS method.

In the future, further research will be carried out, including the consideration of the linkage between external and internal space equipment and their weight distribution.

ACKNOWLEDGEMENTS

This research was supported by the Research Institute of Marine Systems Engineering and Basic Science Research Program through the National Research Foundation of Korea (NRF) funded by the Ministry of Education, Science and Technology (2016R1D11A1A09918294, 2015R1D1A1A01060387).

REFERENCES

Cheng, Y. Z., Y. Wang, Y. Nie, R. Z. Gong, X. Xiong and X. Wang (2012). Design, fabrication and measurement of a broadband polarization-insensitive metamaterial absorber based on lumped elements. Appl. Phys 111, 0449021-04490214.

Fan, Y. N., Y. Z. Cheng, Y. M. Deng and R. Z. Gong (2012). Absorbing Performance of Ultrathin Wide-Band Planar Metamaterial Absorber. IEEE Antennas, Propagation and EM Theory, 672-676.

Goudos, S. K. (2007) A versatile software tool for microwave planar radar absorbing materials design using global optimization algorithms. Materials and Design 28, 2585-2595.

Kim, S. K., G. T. Leem and I. S. Seo (2011). Design of AEM FFS-radom for array antenna. The journal of Korea Electromagnetic Engineering Society 22, 1180-1183 (in Korean, with English Abstract).

Knott, E. F., J. F. Shaeffer and M. T. Tuley (1993). Radar Cross Section (2nd edn), Artech House, Boston·London.

Kwon, H. W., S. Y. Hong, K. K. Lee, J. C. Lee, I. C. Na and J. H. Song (2014b). Analysis of radar cross section for advanced naval vessels. Journal of the Korean Society of Marine Environment & Safety 20, 593-600 (in Korean, with English Abstract).

Kwon, H. W., S. Y. Hong, K. K. Lee, J. C. Lee, I. C. Na and J. H. Song (2014a). Analysis of radar cross section for advanced navy vessels. Journal of the Korean Society of Marine Environment & Safety 20, 593-600 (in Korean, with English Abstract).

Park, H. S., I. S. Choi, J. K. Bang, S. H. Suk, S. S. Lee and H. T. Kim (2004). Optimization design of radar absorbing materials for complex targets. Journal of Electromagnetic Waves and Applications 18, 1105-1117.

Park, T. Y. (2004). A study on RCS prediction code for battleship. Master Thesis, POSTECH (in Korean, with English Abstract).

Richards, M. A. J. A. Scheer and A. H. William (2010). Principles of Modern Radar: Basic principles. Institution of Engineering and Technology.

Saville, P. (2005). A review of radar absorbing material. Defence R & D Canada-Atlantic TM 2005-003.

Shin, H. K., S. G. Lee, D. M. Park, J. W. Shin, M. S. Chung, S. H. Park and Y. B. Park (2017). Analysis of radar cross section of a battleship equipped with an integrated mast module based on PO and PTD. Journal of Electromagnetic Engineering and Science 17, 238-240.

Stratton, J. A. (1941). Electromagnetic Theory. McGraw-Hill, New York.

Wang, Y., Z. Chen, L. Zheng and L. Hao (2017). The application of machine learning in RCS calculation for antenna-radome system. 2017 International Applied Computational Electromagnetics Society Symposium (ACES) Suzhou, 1-2.